

Metamaterial-based wideband electromagnetic wave absorber

Luigi La Spada^{1,3} and Lucio Vegni^{2,4}

¹*School of Electronic Engineering and Computer Science, Queen Mary University of London, London E1 4NS, UK*

²*Department of Engineering, University of Roma Tre, Via Vito Volterra 62, Rome 00146, Italy*

³*l.laspada@qmul.ac.uk*

⁴*lucio.vegni@uniroma3.it*

Abstract: In this paper, an analytical and numerical study of a new type of electromagnetic absorber, operating in the infrared and optical regime, is proposed. Absorption is obtained by exploiting Epsilon-Near-Zero materials. The structure electromagnetic properties are analytically described by using a new closed-form formula. In this way, it is possible to correlate the electromagnetic absorption properties of the structure with its geometrical characteristics. Good agreement between analytical and numerical results was achieved. Moreover, an absorption in a wide angle range (0° - 80°), for different resonant frequencies (multi-band) with a large frequency bandwidth (wideband) for small structure thicknesses ($d = \lambda p/4$) is obtained.

©2016 Optical Society of America

OCIS codes: (160.3918) Metamaterials; (260.2110) Electromagnetic optics.

References and links

1. W. H. Emerson, "Electromagnetic wave absorbers and anechoic chambers through the years," *IEEE Trans. Antenn. Propag.* **21**(4), 484–490 (1973).
2. A. Namai, S. Sakurai, M. Nakajima, T. Suemoto, K. Matsumoto, M. Goto, S. Sasaki, and S. Ohkoshi, "Synthesis of an electromagnetic wave absorber for high-speed wireless communication," *J. Am. Chem. Soc.* **131**(3), 1170–1173 (2009).
3. B. A. Munk, *Frequency Selective Surfaces* (John Wiley & Sons, 2000).
4. M. W. Tsai, T. H. Chuang, C. Y. Meng, Y. T. Chang, and S. C. Lee, "High performance midinfrared narrow-band plasmonic thermal emitter," *Appl. Phys. Lett.* **89**(17), 173116 (2006).
5. E. Knott, J. F. Shaeffer, and M. T. Tuley, *Radar Cross Section*, 2nd ed. (Scitech, Raleigh 2004).
6. E. Popov, D. Maestre, R. C. McPhedran, M. Nevière, M. C. Hutley, and G. H. Derrick, "Total absorption of unpolarized light by crossed gratings," *Opt. Express* **16**(9), 6146–6155 (2008).
7. B. Munk, P. Munk, and J. Pryor, "On designing Jaumann and Circuit Analog absorbers (CA absorbers) for oblique angle of incidence," *IEEE Trans. Antenn. Propag.* **55**(1), 186–193 (2007).
8. N. I. Landy, S. Sajuyigbe, J. J. Mock, D. R. Smith, and W. J. Padilla, "Perfect metamaterial absorber," *Phys. Rev. Lett.* **100**(20), 207402 (2008).
9. B. Zhu, C. Huang, Y. Feng, J. Zhao, and T. Jiang, "Dual band switchable metamaterial electromagnetic absorber," *PIER B* **24**, 121–129 (2010).
10. A. I. M. Ayala, "Metamaterial absorber design and implementation for cruise control radar applications," (Master of Science Thesis, Tufts University, USA, 2009).
11. C. M. Bingham, H. Tao, X. Liu, R. D. Averitt, X. Zhang, and W. J. Padilla, "Planar wallpaper group metamaterials for novel terahertz applications," *Opt. Express* **16**(23), 18565–18575 (2008).
12. H. Tao, C. M. Bingham, A. C. Strikwerda, D. Pilon, D. Shrekenhamer, N. I. Landy, K. Fan, X. Zhang, W. J. Padilla, and R. D. Averitt, "Highly flexible wide angle of incidence terahertz metamaterial absorber: design, fabrication, and characterization," *Phys. Rev. B* **78**(24), 241103 (2008).
13. X. Liu, T. Starr, A. F. Starr, and W. J. Padilla, "Infrared spatial and frequency selective metamaterial with near-unity absorbance," *Phys. Rev. Lett.* **104**(20), 207403 (2010).
14. Y. Avitzour, Y. A. Urzhumov, and G. Shvets, "Wide-angle infrared absorber based on negative index plasmonic metamaterial," *Phys. Rev. B* **79**(4), 045131 (2009).
15. J. Hao, J. Wang, X. Liu, W. J. Padilla, L. Zhou, and M. Qiu, "High performance optical absorber based on a plasmonic metamaterial," *Appl. Phys. Lett.* **96**(25), 251104 (2010).
16. K. Aydin, V. E. Ferry, R. M. Briggs, and H. A. Atwater, "Broadband polarization-independent resonant light absorption using ultrathin plasmonic super absorbers," *Nat. Commun.* **2**(517), 517 (2011).

17. M. H. Li, H. L. Yang, X. W. Hou, Y. Tian, and D. Y. Hou, "Perfect metamaterial absorber with dual bands," *PIER* **108**, 37–49 (2010).
18. H. Tao, C. M. Bingham, D. Pilon, K. Fan, A. C. Strikwerda, D. Shrekenhamer, W. J. Padilla, X. Zhang, and R. D. Averitt, "A dual band terahertz metamaterial absorber," *J. Phys. D* **43**(22), 225102 (2010).
19. X. Liu, T. Tyler, T. Starr, A. F. Starr, N. M. Jokerst, and W. J. Padilla, "Taming the blackbody with infrared metamaterials as selective thermal emitters," *Phys. Rev. Lett.* **107**(4), 045901 (2011).
20. Y. Q. Ye, Y. Jin, and S. He, "Omnidirectional, polarization-insensitive and broadband thin absorber in the terahertz regime," *J. Opt. Soc. Am.* **27**(3), 498–504 (2010).
21. S. Gu, J. P. Barrett, T. H. Hand, B.-I. Popa, and S. A. Cummer, "A broadband low-reflection metamaterial absorber," *J. Appl. Phys.* **108**(6), 064913 (2010).
22. A. Alù, M. G. Silveirinha, A. Salandrino, and N. Engheta, "Epsilon-near-zero metamaterials and electromagnetic sources: tailoring the radiation phase pattern," *Phys. Rev. B* **75**(15), 155410 (2007).
23. M. G. Silveirinha and N. Engheta, "Theory of supercoupling, squeezing wave energy, and field confinement in narrow channels and tight bends using ϵ near-zero metamaterials," *Phys. Rev. B* **76**(24), 245109 (2007).
24. A. Alù, F. Bilotti, N. Engheta, and L. Vegni, "Sub-wavelength planar leaky-wave components with metamaterial bilayers," *IEEE Trans. Antenn. Propag.* **55**(3), 882–891 (2007).
25. A. Vakil and N. Engheta, "One-atom-thick reflectors for surface plasmon polariton surface waves on graphene," *Opt. Commun.* **285**(16), 3428–3430 (2012).
26. P. B. Johnson and R. W. Christy, "Optical constants of the noble metals," *Phys. Rev. B* **6**(12), 4370–4379 (1972).
27. J. Gómez Rivas, C. Janke, P. Bolivar, and H. Kurz, "Transmission of THz radiation through InSb gratings of subwavelength apertures," *Opt. Express* **13**(3), 847–859 (2005).
28. W. G. Spitzer, D. Kleinman, and D. Walsh, "Infrared properties of hexagonal silicon carbide," *Phys. Rev.* **113**(1), 127–132 (1959).
29. A. H. Sihvola, *Electromagnetic Mixing Formulas and Applications* (Institution of Electrical Engineers, 1999).
30. Y. Jin, S. Xiao, N. A. Mortensen, and S. He, "Arbitrarily thin metamaterial structure for perfect absorption and giant magnification," *Opt. Express* **19**(12), 11114–11119 (2011).
31. S. Feng and K. Halterman, "Coherent perfect absorption in epsilon-near-zero metamaterials," *Phys. Rev. B* **86**(16), 165103 (2012).
32. S. Zhong and S. He, "Ultrathin and lightweight microwave absorbers made of mu-near-zero metamaterials," *Sci. Rep.* **3**(2083), 2083 (2013).
33. S. Tretyakov, "On geometrical scaling of split-ring and double-bar resonators at optical frequencies, Metamaterials," *Metamaterials (Amst.)* **1**(1), 40–43 (2007).
34. K. Halterman, S. Feng, and V. C. Nguyen, "Controlled leaky wave radiation from anisotropic epsilon near zero metamaterials," *Phys. Rev. B* **84**(7), 075162 (2011).
35. M. Abramowitz and I. Stegun, *Handbook of Mathematical Functions* (Dover Publications, 1964).
36. G. V. Naik, J. Kim, and A. Boltasseva, "Oxides and nitrides as alternative plasmonic materials in the optical range," *Opt. Mater. Express* **1**(6), 1090–1099 (2011).
37. H. Caglayan, S.-H. Hong, B. Edwards, C. R. Kagan, and N. Engheta, "Near-infrared metatronic nanocircuits by design," *Phys. Rev. Lett.* **111**(7), 073904 (2013).
38. CST STUDIO SUITE™ (CST of Europe Inc. 2014), www.cst.com.
39. Y. R. Padooru, A. B. Yakovlev, C. S. R. Kaipa, G. W. Hanson, F. Medina, F. Mesa, and A. W. Glisson, "New absorbing boundary conditions and analytical model for multilayered mushroom-type metamaterials: applications to wideband absorbers," *IEEE Trans. Antenn. Propag.* **60**(12), 5727–5742 (2012).

1. Introduction

In recent years, there has been an increasing interest in the area of electromagnetic wave absorbers. An electromagnetic absorber is a designed device that can inhibit the reflection (or the transmission) of the electromagnetic energy. Today, absorbers are crucial in several application fields: to reduce the antenna side lobe radiation [1], to absorb the electromagnetic interferences [2], for radar cross section reduction [3], or to develop selective thermal emitters [4]. The main and early interest in electromagnetic absorbers can be found in the microwave regime. Different kinds of absorbers have been implemented: the Salisbury screen, the Jaumann absorber [3], the Dallenbach layer [5], the crossed grating absorbers [6] and the circuit analog ones [7].

Despite such a plethora of devices, several issues are still present. First of all, the thickness: most of the above mentioned solutions require the thickness to be at least $\lambda/4$, where λ is the free-space wavelength at the resonant frequency. Secondly, it is difficult to control the specific absorption properties, due to the fact that it is not easy to find materials naturally impedance matched to free space. Finally, the restricted operative frequency range:

the aforementioned electromagnetic wave absorbers are typically developed in the microwave regime.

Recently, the advent of metamaterials allows overcoming such issues. Numerous researches suggest a growing role for metamaterials as novel tools to develop electromagnetic wave absorbers, in the microwave, infrared and optical frequency range. Metamaterials permit to overcome limits that with conventional materials were considered insuperable. Their extraordinary characteristics derive from the possibility to design their effective electromagnetic parameters (electrical permittivity ϵ and magnetic permeability μ) to obtain specific required properties.

Numerous experimental and numerical works on metamaterial-based absorbers can be found in literature. To have a complete view, we have to classify them for the different ranges of the electromagnetic spectrum. For what concerns the microwave region, they are typically implemented in array configurations with different particle geometries as unit-cell: metal wires [8], magnetic or electric resonators [9]. In such structures the absorption mechanism can be described by the coupling between the incident electric and/or magnetic field and the resonators themselves. In general, they demonstrated good absorption results close to the unity, up to high angle of incidence. Same results were achieved in the millimeter [10] and in the THz regime [11] especially for a wide angle range [12]. By scaling the dimensions of the unit cell and changing the geometry used, it was possible to obtain good results also in the mid-Infrared [13] and Infrared [14] regions, respectively. In this case the absorption is obtained due to plasmons trapped under the metallic structures. Instead, in the near-Infrared wavelengths region, another phenomenon is exploited to achieve absorption: the local excitation of the magnetic/electric dipolar plasmonic resonances between nanoparticles and metallic ground plane [15].

The visible regime represents a challenge; as a consequence experimental realizations in this region are not as many as in the previous cases. Recently, a broadband absorption in the visible spectrum was achieved in [16].

Other important issues, related to a good absorber, are the multi-band behavior and the operating frequency bandwidth. Multiple resonant structures can be obtained by using two or more separately resonating elements in the same array [17] or different sections of a single element that resonate at different frequency [18]. Instead, a broad resonant peak can be reached by using multiple resonating inclusions (whose frequencies are really close each other) in a single unit cell [19], by stacking multiple layers in which resonators share the same ground plane [20], or by incorporating lumped elements into the resonator [21].

From what we have seen so far, the major issues in electromagnetic absorber design concern satisfying the following requirements:

- Small thickness: most of the presented absorbers require a thickness at least around $\lambda/4$
- Broad angle range: the absorption is required at all angle of incidence
- Broad bandwidth and multi-resonant behavior: wide the bandwidth of the single resonant frequency and/or create multiple resonant bands with the wider bandwidth possible
- Scaling the structure: the possibility to replicate the same behavior and performances in all the electromagnetic spectrum frequency ranges.

The main goal, not easily achievable, is to satisfy all the features listed above at the same time.

Recently, several studies focused their attention on a particular kind of metamaterials entitled Epsilon-Near-Zero (ENZ) and on their particular electromagnetic properties. Such materials, characterized by low (mostly near zero) values of the real part of the relative permittivity, have several interesting applications such as tailoring the phase-front [22], confining electromagnetic fields [23], enhancing transmission [24], and focusing [25].

ENZ materials can be found pretty easily in nature. A well-known example is an electron gas, characterized by a Drude-type dispersion model, which near its plasma frequency has permittivity near zero. In the same way, at infrared and optical frequencies some low loss noble metals, such as silver and gold [26], semiconductors [27], and polar dielectrics [28] may behave as ENZ materials near their plasmas frequencies. When such materials are not present naturally, they can be fabricated at a desired frequency as metamaterials by embedding specific inclusions in a host medium [29].

Recent evidence suggests that good absorption could be obtained by ENZs and Mu-Near-Zero (MNZs) with low loss [30], thin anisotropic ENZ metamaterials [31] and high losses MNZ materials [32].

Considering all these issues, in this paper, by exploiting the particular properties of ENZ materials we propose the design of an electromagnetic wave absorber. The purpose of this paper is to satisfy all the mentioned requirements at the same time. Thus the paper's central research objective is to obtain a good absorption level for different angles of incidence, at single and/or different resonant frequencies with the wider bandwidth possible, for small layer thicknesses.

The article is structured as follows: first of all, the general operation pattern is presented and analytically described by the use of the Transmission Line Theory. This provides us the possibility to correlate the electromagnetic properties of the structure with its geometrical characteristics. Then a description of the main important features of the ENZ absorber is reported. Finally, two different design solutions are presented: a multilayer structure and a metasurface-based device implementation, respectively.

2. The ENZ absorber analytical model

The structure under study is shown in Fig. 1(a). An isotropic ENZ material slab with a thickness d is placed on top of an infinitely extended Perfect Electric Conductor (PEC) sheet. The top layer and the ENZ slab are entitled as region 1 and region 2, respectively. Let's assume the region 1 as free space with electric permittivity ϵ_0 and magnetic permeability μ_0 . The ENZ material is described by the electric permittivity $\epsilon_{\text{ENZ}}(\omega) = \epsilon_0(\epsilon_r(\omega) - j\epsilon_i(\omega))$ and magnetic permeability $\mu_{\text{ENZ}} = \mu_0\mu_r$ with $\mu_r = 1$ the relative magnetic permeability of the free space and $\omega = 2\pi f$ is the frequency (rad/s). The material in the ENZ region in terms of permittivity can be described by the following Drude model:

$$\epsilon_{\text{ENZ}} = 1 - \frac{\omega_p^2}{\omega^2 - j\omega\gamma} \quad (1)$$

being $\omega_p = 2\pi f_p$ the plasma frequency and γ the damping frequency.

It is well established that at microwave frequencies metals can be considered as PEC, instead by increasing the frequency, the thickness of the metal can no longer be neglected and metals are not ideal conductors any more [33]. At such frequencies, metals exhibit some losses and a dispersive behavior which can be represented in a given frequency range by the aforementioned Drude model [34]. In this work the PEC was chosen (instead of real metal) to simplify the analytical approach. Moreover, in [31] was shown that the transmittance of the interface ENZ-silver is near zero (around 10^{-10}). In other words, the silver layer (underneath the ENZ material) can be either real metal or PEC.

The structure is excited by an electromagnetic plane wave, having the electric field and the propagation vector \mathbf{k} inclined to the ground plane with a generic Angle Of Incidence (AOI) α , as depicted in Fig. 1(a).

By using the Transmission Line Theory (TLT) we developed an analytical approach to find the reflection coefficient r . This leads to the control of the absorption properties through the design of subwavelength materials using TLT, which is accurate and efficient. In this way the manipulation and control is no longer limited only to a single frequency but can be

extended to a broad range of frequency spectrum. In addition, the proposed approach can be applied to a broad range of materials and it can be extended to design them with arbitrary shapes and dimensions.

In order to develop the analytical model, we consider each layer as a section of the transmission line, each of one characterized by their impedances, as depicted in Fig. 1(b). In particular, $Z_0 = \eta \cdot \cos(\alpha)$ is the impinging wave impedance, dependent on the angle of incidence α with η the free space characteristic impedance ($\eta = 120\pi$). Z_{ENZ} is the impedance of the ENZ material, the PEC layer is represented by a short circuit.

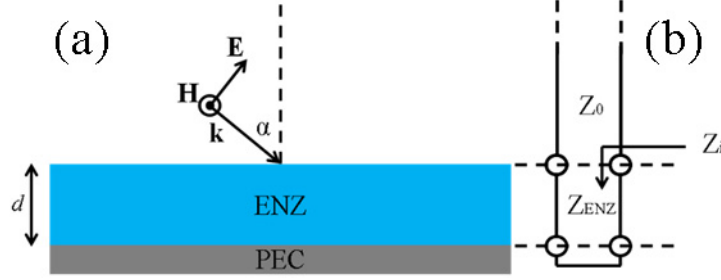


Fig. 1. (a) A plane wave impinges (with an angle α) on an isotropic ENZ (thickness d) - PEC bilayer; (b) Equivalent transmission line model.

In this case, due to the presence of the PEC, the transmission coefficient T is zero, so the corresponding absorption A is related to the reflection coefficient r as $A = 1 - |r|^2$. As a consequence the absorption is obtained when the coefficient r approaches to 0.

First of all we calculate the input impedance at the interface between air and the ENZ layer:

$$Z_i = \frac{\eta}{\sqrt{\epsilon_{ENZ}}} \sqrt{1 - \frac{\sin^2(\alpha)}{\epsilon_{ENZ}}} \tan\left(\frac{\omega}{c} \sqrt{\epsilon_{ENZ}} d\right) \quad (2)$$

Then, we calculate the reflection coefficient by using the relation:

$$r = \left| \frac{Z_i - Z_0}{Z_i + Z_0} \right|^2 \quad (3)$$

where Z_i is the total impedance of the ENZ and the PEC.

After some mathematical manipulations [35], the corresponding reflection coefficient formula can be expressed as:

$$r = \frac{-at^3 + bt^2 + c}{at^3 + bt^2 + c} = 1 - \frac{2at^3}{at^3 + bt^2 + c} \quad (4)$$

being $t = d/\lambda_p$ (where λ_p the ENZ material plasma wavelength) and the coefficients:

$$\begin{aligned} a &= \pi \arctan\left(\frac{\epsilon_i}{\epsilon_r}\right) \cos(\alpha) \\ b &= 1 - 2\pi\epsilon_r \cos^2(\alpha) \sqrt{\epsilon_r^2 + \epsilon_i^2} \\ c &= \cos^2(\alpha) \sqrt{\epsilon_r^2 + \epsilon_i^2} \end{aligned} \quad (5)$$

The derived analytical model is crucial to design the structure in according with specific requirements for accurate and efficient design of electromagnetic wave absorbers. In

particular, the formulas are developed to relate the propagation characteristics of the impinging wave with both electromagnetic and geometric properties of the structure. Specifically, the (4) provides a powerful tool in order to link the absorption properties of the device (in terms of amplitude, magnitude and resonant frequency), to the electromagnetic ENZ material ones (ϵ_r and ϵ_i), the angle of incidence (α) and the thickness d of the ENZ layer.

3. The absorption mechanism

As shown in Eq. (4) the reflection coefficient is a function (not simple) of: frequency, angle of incidence α , real/imaginary part of the ENZ material permittivity and thickness d . By using the analytical models proposed, it is possible to study the effect of the geometrical (Angle Of Incidence (AOI) α and thickness d) and the electromagnetic parameters of the ENZ layer (electric permittivity in its real and imaginary part ϵ_r and ϵ_i , respectively) on the absorption characteristics of the structure. To describe the behavior of the structure under study with real materials, the Drude-like dispersive permittivity models for Aluminum Zinc Oxide (AZO, $f_p = 193\text{THz}$), Gallium Zinc Oxide (GZO, $f_p = 217\text{THz}$) and Indium Tin Oxide (ITO, $f_p = 210\text{THz}$) have been used [36, 37]. The structure absorption properties at different AOI, are evaluated for the following ENZ slab thicknesses: $d/\lambda_p = 0.05$, $d/\lambda_p = 0.1$, $d/\lambda_p = 0.15$, $d/\lambda_p = 0.2$ and $d/\lambda_p = 0.25$

Figure 2 shows the reflection coefficient r (color) plotted in a 2D domain of the AOI (degrees) and frequency (THz) for fixed thickness ratios d/λ_p of GZO (ENZ region for $190\text{ THz} < f < 260\text{ THz}$). The dispersion behavior for GZO is plotted in Fig. 2(e). Similar results can be achieved by using other materials, such as AZO and ITO.

It is apparent from this data set that, for small thicknesses ($0.05 \leq d/\lambda \leq 0.1$), the best absorption possible is reached only for very small angle range ($50^\circ \leq \alpha \leq 70^\circ$). By increasing the thickness ($d/\lambda \geq 0.2$) two regions are present, in particular referring to Fig. 2(c), one (Region a) in the ENZ region and the other one (Region b) nearby it.

For larger thicknesses ($d/\lambda \geq 0.25$) the two regions are already present, but they collapse in one. As a consequence the absorption is obtained for a larger AOI range ($0^\circ \leq \alpha \leq 60^\circ$). Beyond the 80° the absorption is no longer significant.

For normal incidence the reflection coefficient is reduced only when the thickness is large. This can be explained in the following way. From boundary conditions at the interface AIR-ENZ we have the continuities of the tangential components $E_{1t} = E_{2t}$, instead the normal components are related in the following manner $\epsilon_1 E_{1n} = \epsilon_2 E_{2n}$ across the separation surface. At the interface ENZ-PEC we have the zero-tangential component of the electric field condition on the PEC plate surface. As a consequence, the most interesting result, is that at normal incidence ($\alpha = 0$) the absorption can be exclusively attributed to the presence of both high losses and large thicknesses of the ENZ material. In this case the only component of the electric field is purely longitudinal and it doesn't affect the absorption.

Instead, for all the other AOI $\alpha > 0$ a normal component of the electric field exists inside the ENZ layer. Such component is magnified by the ENZ layer. It is well known from boundary condition for the normal component that $E_{2n} = (\epsilon_1/\epsilon_2) \cdot E_{1n}$, where $\epsilon_1 = 1$ and $\epsilon_2 \rightarrow 0$. As a consequence, when the normal component of the electric field is present, to obtain a good absorption thin thicknesses can be used.

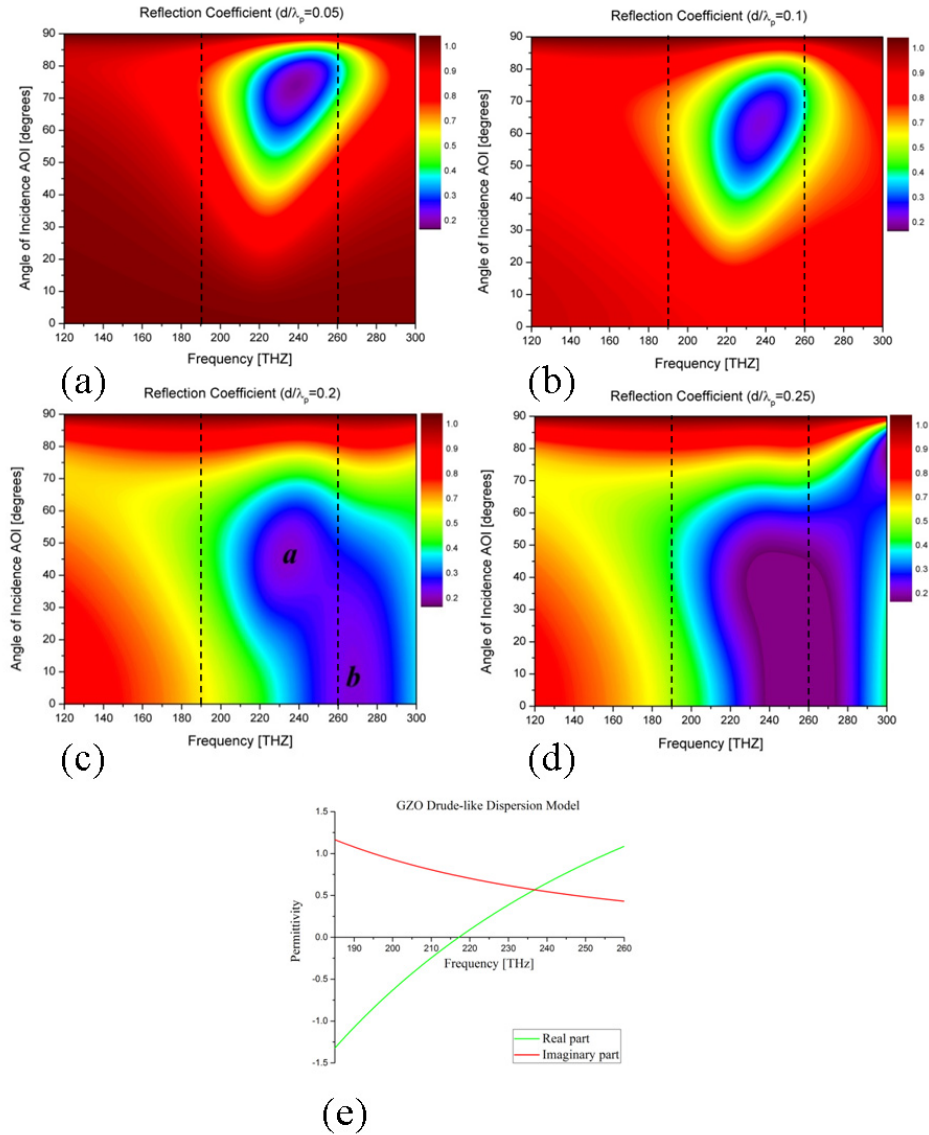


Fig. 2. Reflection coefficient as a function of AOI (degrees) and frequency (THz) of GZO ($f_p = 217$ THz) for: (a) $d/\lambda_p = 0.05$, (b) $d/\lambda_p = 0.1$, (c) $d/\lambda_p = 0.2$, (d) $d/\lambda_p = 0.25$, (e) GZO Permittivity Dispersion Behavior.

As mentioned above the reflection coefficient (consequently, the absorption) is also related to the ENZ electromagnetic characteristics.

It is well known that the resonant frequency of the reflection is related to the real part of the permittivity (ϵ_r) of the ENZ slab, instead the magnitude and the amplitude width of the reflection is related to the imaginary part (ϵ_i).

The correlation between r and ϵ_i is worth mentioning because, as expected, the reflection coefficient decreases when the ENZ losses grow. In this case, the absorption is relevant only for larger thicknesses, as also confirmed by Eq. (4).

In particular, for normal incidence the reflection coefficient is at its minimum only when a large imaginary part of the ENZ material comes into play. Instead, for the $\text{AOI} > 0$:

- In the maximum absorption areas (as also shown in Fig. 2) the real part is comparable (same magnitude order) to the imaginary one. In this case, the absorption is larger compared to the previous cases, as also confirmed by Eq. (4).
- The angle range, to which the greatest absorption is reached, is a function of the imaginary part (ϵ_i)

4. ENZ-based absorbers design

Research has tended to focus on designing highly lossy structures to reach the best absorption. This is not a big deal in the microwave range, where thin structures with a large imaginary part can be implemented easily. One of the major drawbacks considering infrared and/or optical frequencies is that materials have very low losses compared to the ones in the microwave range. This represents an important limitation in designing a good absorber: as a consequence in order to achieve a great absorption, a greater ENZ layer thickness is necessary. Our goal is to obtain absorption for different AOI and a wide resonant frequency band by using thin thicknesses.

In the following two alternative solutions, in order to overcome such a problem, are proposed: a multi-layer structure and a metasurface-based structure. Both solutions rely on the concept of confining the electric field in ENZ region, to exploit the absorption mechanism aforementioned.

Simulations are performed by using a frequency domain solver, implemented by the finite integration commercial code CST Microwave Studio [38].

4.1 The multi-layer structure

In [39] the reflection characteristics of a multilayer mushroom structure with thin material patches for new wideband absorbers is developed. By following a similar procedure, let's consider a 3-layered structure depicted in Fig. 3 (a): a combination of High Permittivity Value (HPV) dielectrics and ENZ material. At the first interface HPV – ENZ: if the dielectric material with high permittivity value is the layer 1 (n_1 is really large) and the ENZ material is the layer 2 ($n_2 \rightarrow 0$), we have (by applying the Snell's law): $\sin(\theta_2) = (n_1 / n_2) \cdot \sin(\theta_1)$. As a consequence, for any angle of incidence α (not zero), exists always a normal component of the electric field in the ENZ layer (see Fig. 3 (b)). At the interface ENZ – HPV the ray curves towards the normal axis (dashed line), by applying the boundary condition we have that the normal component is still greater in the ENZ layer (see Fig. 3 (b)): $E_{2n} = (\epsilon_{HPV}/\epsilon_{ENZ}) \cdot E_{3n}$. In other words, the presence of the HPV, and consequently the huge contrast in the permittivity values, is crucial not only to ensure the presence of a normal electric field component, but also to confine the electric field in the ENZ layer.

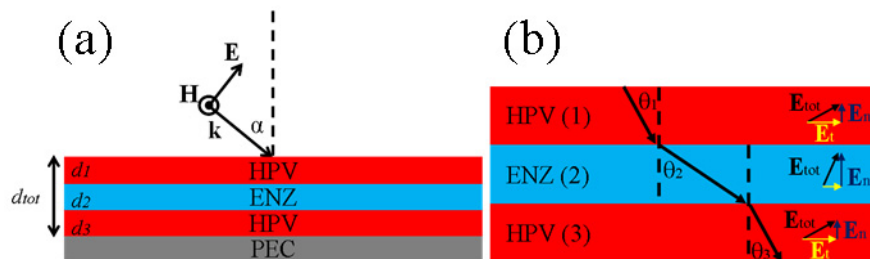


Fig. 3. Multi-layer device: (a) side-view, (b) Snell's law for multi-layer structure.

Results are reported in Fig. 4 for the AZO material. Similar results can be obtained with the other two materials (GZO and ITO). Let us fix the good absorption criteria when the resonant tip reaches the value of -10 dB. From Fig. 4(a) it is possible to note how absorption

is achieved at all angles, from 0° to 80° ; in particular at the same frequency in the angle range 0° - 30° and for $\alpha > 30^\circ$ the central resonant frequency blue shifts and the bandwidth enlarges (40° - 70°).

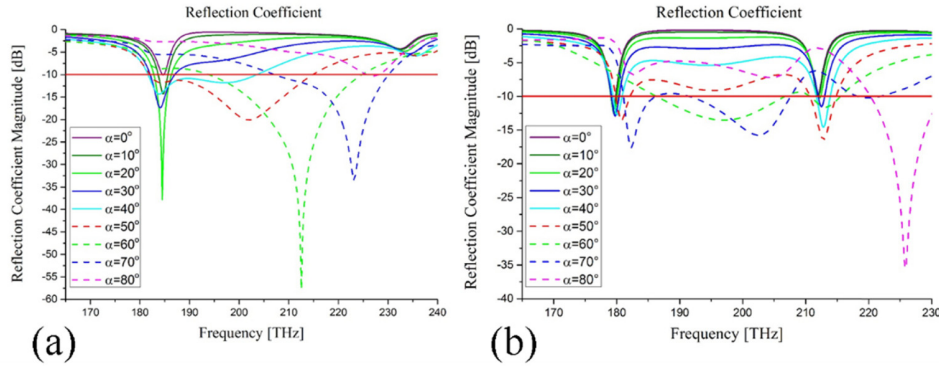


Fig. 4. Absorption properties for the 3-layered structure: (a) multi-frequency and wideband behavior ($d_{10}/\lambda_p = 0.25$); (b) multi-band behavior ($d_{10}/\lambda_p = 0.5$, with $d_1/\lambda_p = 0.05$, $d_2/\lambda_p = 0.2$, $d_3/\lambda_p = 0.25$)

By managing the thickness of the three different layers it is possible to reach absorption also at different resonant frequencies in the ENZ region of the material. An example for multi-band absorption is shown in Fig. 4(b). For AOI in the range 0° - 50° two different absorption frequencies are present; instead for $\alpha > 50^\circ$ the absorption bandwidth enlarges significantly.

4.2 The metasurface-based structure

The structure under study is shown in Fig. 5(a). In addition to the structure considered in Fig. 1(a), on the ENZ slab a metasurface is deposited. It consists of planar array of resonant metallic cross-shape structure, as depicted in Fig. 5(b). The reason to choose such a geometry is due to the fact that, the resonator can be excited by both the electric and magnetic field.

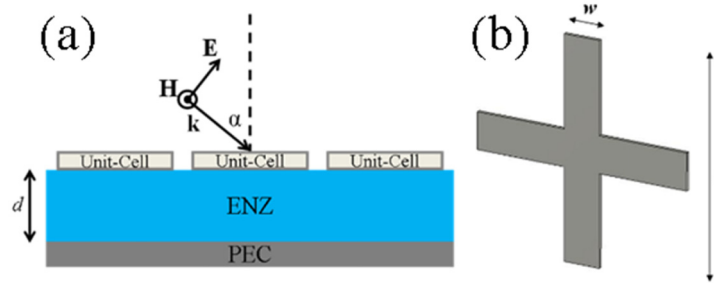


Fig. 5. Metasurface-based electromagnetic absorber: (a) Side-View, (b) Unit-Cell.

The metal inclusion, tuned to resonate in the ENZ region of the substrate material, permits to create additional electric field, not present before, between the strip and the ground plane.

In Fig. 6 the reflection coefficient spectra for the proposed structure in the TE case and TM case is presented for the AZO material. Similar results can be obtained with the other two materials (GZO and ITO). It is possible to note how absorption is achieved at all angles, from 0° to 80° ; in particular at the same frequency in the angle range 0° - 30° and for $\alpha > 30^\circ$ the central resonant frequency blue shifts and the bandwidth enlarges (40° - 70°). It is interesting to note that for $\alpha > 30^\circ$ new absorption resonant frequencies (in the ENZ region and outside)

arise. It confirms the possibility to use the structure as a multi-band electromagnetic wave absorber.

The main advantages in using the combination of metasurface and ENZ are the following:

1. *Absorption at normal incidence:* Even though at $\alpha = 0$ the electric field component is purely longitudinal, due to the creation of additional electric field in the ENZ substrate layer at the resonance, a strong absorption can be achieved.
2. *Independence to impinging polarization:* the structure resonates with both linear TE and TM electromagnetic waves.
3. *Rotational symmetry:* the structure allows us to obtain absorption for oblique incidence up to 80° and for circular polarized impinging electromagnetic waves.

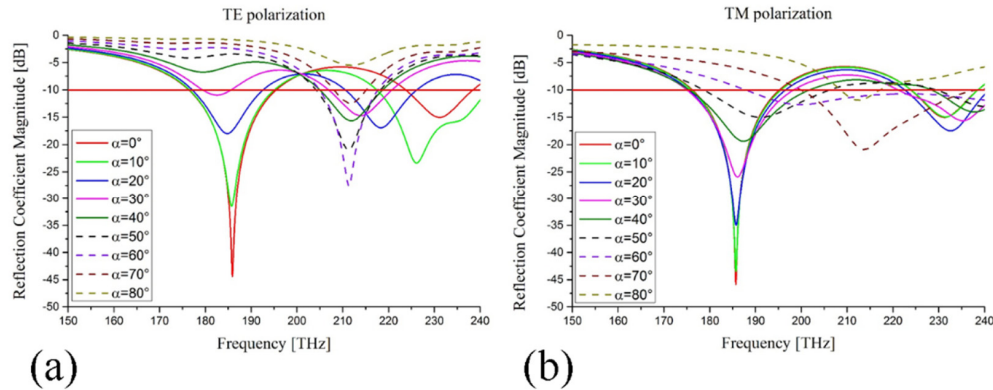


Fig. 6. Absorption properties for the metasurface-based structure: (a) TE polarization and (b) TM polarization.

5. Conclusions

This paper investigated the potential role of ENZ materials to design a new electromagnetic absorber. Such a material, thanks to their peculiar properties, path new ways forward the design of electromagnetic absorbers, satisfying specific requirements.

In this regard, first of all by using the Transmission Line Approach, a new analytical model, describing the electromagnetic absorption characteristics of the structure (in terms of magnitude, bandwidth and frequency position) is presented. The properties of the absorber were discussed.

In addition to this, in order to enhance the absorption properties of the device, two possible designs were developed: a multi-layered configuration and a metasurface-based structure. In both cases, full-wave simulations have confirmed the ability of the proposed configuration to behave as a multi-band and broadband absorber in a wide range of angle of incidence ($0^\circ - 80^\circ$) for small thicknesses.

The proposed structure offers great potential in a wide variety of practical application fields such as to build-up selective thermal emitters, for detection and sensing, for imaging and defense applications.

Acknowledgments

The authors thank prof. N. Engheta (University of Pennsylvania, Philadelphia, USA) for the useful discussion and suggestions on this subject.